JOURNAL OF MATERIALS SCIENCE 33 (1998) 3145–3149

Degradation behaviour of a composite material for thermal protection systems
Part II *Process simulation*

L. TORRE, J. M. KENNY
Institute of Chemical Technology, University of Perugia, Loc. Pentima bassa, 05100, Terni, Italy
E-mail: terrel@unipg.it

A. M. MAFFEZZOLI
Department of Materials Science, University of Lecce, Via per Arnesano, 73100, Lecce, Italy

Mass and energy balance equations have been solved in order to simulate the behavior of a silicon-based ablative composite used as a thermal protection shield for a non-animated space capsule. A method to calculate some of the parameters in the energy balance equation, is proposed, taking advantage of combined thermal analysis techniques. Furthermore, degradation kinetics in the hypothesis of constant volume is used to solve the mass balance. The results of the computer simulation are compared with the experimental data, obtained using plasma arc testing. The model can be used for both material selection and thickness calculation for thermal protection shields. ©*1998 Kluwer Academic Publishers*

1. Introduction

In Part I [1], the kinetic characterization of an ablative material was analysed. In order to study the overall ablative behaviour of a thermal shield, the developed degradation model must be coupled with energy and mass balance. The aim of the mathematical model was to predict the temperature and the density evolution when an ablator is subjected to high heat fluxes. The problem can be divided in two parts: (a) prediction of the bulk behaviour, (b) specification of the boundary conditions at the material surface.

First, this work will focus on the problems relative to the thermal degradation and heat exchange, and some approximations will be made in order to make the problem feasible.

Second, the boundary layer phenomenology is considered for a quasi steady ablation, taking into account the mass and thermal diffusion and the chemical reaction occurring in the layer. Quasi steady problems are those in which the wall temperature, the velocity of the degrading front, and the temperature profile with respect to the degrading front, are constant. In these processes, the material bulk is only affected by heat exchange, while in the boundary layer, chemical reactions and diffusion are occurring [2–5]. When the external conditions change very rapidly with time, the reactions occurring within the bulk are assumed to be the most important and must be taken into account at every instant.

Fig. 1 shows a schematic illustration of the ablation in a shield layer. In this case, the process is a transitory regime problem, where the material undergoes pyrolysis and the degraded front moves into the bulk. The material can then be divided into three zones: one containing the unreacted material; one in which the pyrolysis is effectively taking place, producing gases; and one that is formed by the char and the reacted gases, in which no reactions occur. Of course, this simple scheme can be complicated by many factors. For example, the reacted gases can further react with each other or with the char, the char can be destroyed as effect of thermal stress or mechanical damage, and further unpredicted reaction can take place.

Nevertheless, in this simplified analysis, the overall phenomena will be described with a simple reaction pattern:

$$\text{unreacted material} \rightarrow \text{char} + \text{reacted gases}$$

Although this approach is very simplified, it describes most of the main processes occurring in an ablative layer, allowing comparison of the thermal performances of different ablative materials.

Furthermore, this mathematical model has been compared with the experimental temperature measured during a simulation of the ablation process in a plasma torch facility.

2. Experimental procedure

Equipment capable of simulating the aerodynamic heating occurring during space re-entry must be able to provide a high-speed and high-temperature gas flow on the test sample. All methods of simulation of the ablation process are based on the same principle

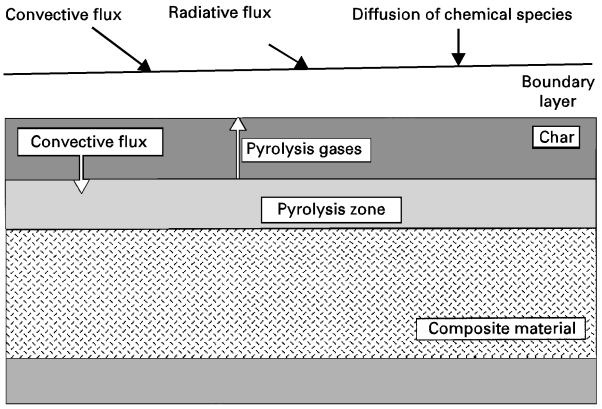

Figure 1 Schematic illustration of the ablation process.

[6]: a sample with a defined geometry is hit by a hot stream whose enthalpy is known, while the temperature inside the sample is measured at different depths. The differences between the different methods lies in the way the heat flux is created. When the stream is created by a flux of burning gases the method is called a gas flame test; when a beam is created by a high-temperature arc, the method is called an arc image test. In this study, a plasma arc test was used. A plasma arc device creates a high-temperature ionized gas stream by streaking an arc between two electrodes and injecting the working gases. This test represents one of the better simulations of the working condition of an ablator, producing high heating rates and allowing measurement of the enthalpy of the heat flux, and of the stagnation pressure. The equipment used is able to provide a heat flux up to 700 $kW\,m^{-2}$ creating a stagnation pressure on the sample of 500 torr (1 torr = 133.322 Pa) with a plasma of argon, and air as working gas. It works in a conventional vacuum chamber in which are two arms, on one of which the sample holder is positioned, and on the other is a calorimeter sensor able to measure the stream enthalpy. Both arms can be rotated and exposed to the high-temperature plasma. The samples were of cylindrical shape with 3.5 cm diameter and 2 cm thick as shown in Fig. 2. The ablative material is then exposed to the stream for a period of time from 100–350 s.

During the test, once the plasma stream was created, the calorimeter was first exposed in order to evaluate the enthaply of the stream, then the arm with the sample was rapidly placed in the same position as the calorimeter under the plasma stream. The sample holder was provided with three thermocouples that were placed inside the sample, each at a certain depth in order to measure the temperature profile as a function of the exposure time, inside the sample. Owing to the high-temperature gradients inside the exposed sample, it was very important to know the exact position of the thermocouples. A small deviation from the real position caused, in fact, a large error in the determination of the temperature. Therefore, the sample was sectioned after each test and the exact position of the thermocouple was then remeasured. A section of a test sample is shown in Fig. 3.

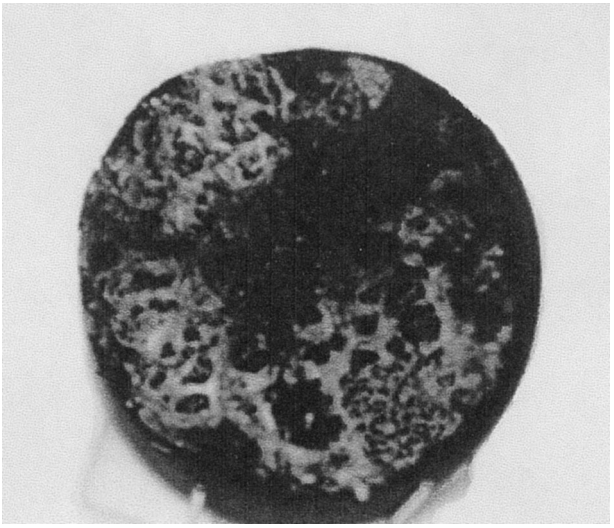

Figure 2 Photograph of the arc test sample.

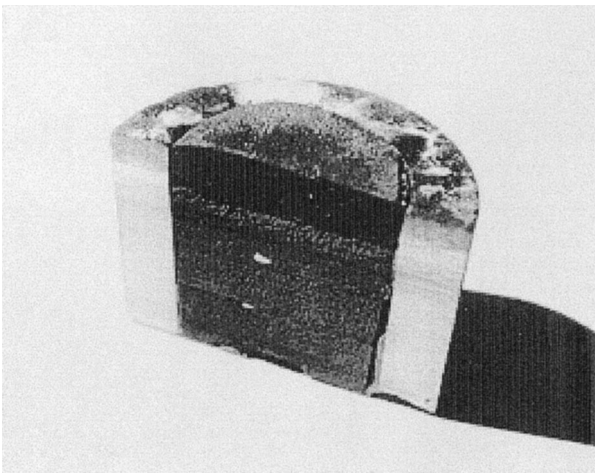

Figure 3 Section of the tested sample.

3. Mathematical modelling of the thermal behaviour of ablative materials

3.1. Heat conduction

Bearing in mind the scheme given in Fig. 1, some assumptions can be made in order to simplify the modelling of heat through a thermal shield. The first assumption is to consider heat flow only in the direction normal to the surface (y-axis). The second assumption is that the gases coming out of the bulk are in thermal equilibrium with the char, i.e. the bulk and the char are at the same temperature, chemical reactions between the char and the gases coming out are neglected.

3.2. Mass balance

Even in the mass balances some simplifying considerations have to be made. A control volume must be chosen to derive the mass balance equations, and the cross-sectional area must be considered constant with the normal distance y. This situation does not represent the actual problem well, because space vehicle surfaces are generally cylindrical surfaces and are a function $S = S(y)$, where S is the cross-sectional area.

Assuming the mass of the outcoming gases to be negligible, because their mass is generally much smaller than the mass of the solid material, and assuming that every point of the control volume has a very short gas residence time, the conservation of mass is expressed by the following equation [7, 8]

$$\left(\frac{\partial \dot{m}g}{\partial y}\right) = \frac{\partial}{\partial t}(\rho S) = S\left(\frac{\partial \rho}{\partial t}\right) + \rho\left(\frac{\partial S}{\partial t}\right) \tag{1}$$

where ρ is the density of the unreacted material, mg is the local mass flux, and S is the cross-sectional area. From the above assumption, the cross-sectional area is only a function of the distance y

$$\left(\frac{\partial S}{\partial t}\right) = 0 \tag{2}$$

The mass conservation equation then becomes

$$\left(\frac{\partial \dot{m}g}{\partial y}\right) = S\left(\frac{\partial \rho}{\partial t}\right) \tag{3}$$

In Equation 3 the term mg represents the mass flux, and its time derivative represents the rate of gas production. The total gas flux can be obtained by integrating Equation 3

$$\dot{m}g = \int_{y}^{yb} S\left(\frac{\partial \rho}{\partial t}\right) \mathrm{d}y \tag{4}$$

The following model is then used to define the density and the rate of density variation. Let us consider that the non-reacted composite is formed by three different elements that undergo independent decomposition, in this schematic model, the resins are considered to be composed by two degrading elements indicated by a, and b. This assumption allows one to consider different resins with different decomposition reaction, the letter c refers to the reinforcement. With this scheme the density will assume the following value

$$\rho = \Gamma(\rho_a + \rho_b) + (1 - \Gamma)\rho_c \tag{5}$$

where Γ is the volume fraction of the resin. Allowing the volume fraction of the resin to vary, as well as the term ρ_a and ρ_b, several materials can be considered, making this relation completely general.

The density variation rate can then be obtained, deriving Equation 5 in respect of the time at constant y

$$\left(\frac{\partial \rho}{\partial t}\right)_y = \Gamma\left(\frac{\partial \rho_a}{\partial t} + \frac{\partial \rho_b}{\partial t}\right)_y + (1 - \Gamma)\left(\frac{\partial \rho_c}{\partial t}\right)_y \tag{6}$$

Evaluating the degradation kinetics of all the elements, a, b, and c, allows the calculation of the density changes.

3.3. Conservation of energy

The following functions will be considered in the energy balance for enthalpy, temperature and density, respectively: $h = h(T\,\rho)$, $T = T(y, \rho)$, $\rho = \rho(y, t)$.

The differential equation that expresses the conservation of energy will contain a term indicating the accumulation, one conductive term, and one convective term [5, 9, 10]

$$\frac{\partial}{\partial t}(\rho h S)_y = \frac{\partial}{\partial y}\left(kS\frac{\partial T}{\partial y}\right)_t + \frac{\partial}{\partial y}(mgh_g)_t \tag{7}$$

where h_g is the enthalpy of the out coming gases.

The left-hand side of Equation 7 can be modified in the following manner

$$\frac{\partial}{\partial t}(\rho h S)_y = \rho h \frac{\partial}{\partial t}(S)_y + S\frac{\partial}{\partial t}(\rho h)_y \tag{8}$$

To express the rate of enthalpy variations a function of temperature and density, a schematic model has to be developed. A reasonable assumption is to consider that the partially pyrolysed material is a blend of completely reacted and completely unreacted material. This can be done by introducing a parameter ε_p which expresses the volume fraction of the unreacted material in a control volume. This parameter is equal to one when no material has yet reacted, and equal to zero for the char. The density can then be expressed by

$$\rho = \varepsilon_p\rho_p + (1 - \varepsilon_p)\rho_c \tag{9}$$

where the subscripts p and c refer to the unreacted material and the char, respectively.

The total enthalpy can then be expressed as

$$\rho h = \varepsilon_p\rho_p h_p + (1 - \varepsilon_p)\rho_c h_c \tag{10}$$

The term h_p and h_c can be expressed as

$$h_p = h_p^0 + \int_0^T Cp_p \mathrm{d}T \tag{11}$$

$$h_c = h_c^0 + \int_0^T Cp_c \mathrm{d}T \tag{12}$$

In these equations, T is the temperature, Cp is the specific heat, h_p^0 is the enthalpy of unreacted material formation, and h_c^0 is the enthalpy of char formation. Taking the derivative of Equation 10 with respect to the time we get

$$\frac{\partial(\rho h)}{\partial t} = \rho_p h_p \frac{\partial \varepsilon_p}{\partial t} + \rho_p\varepsilon_p \frac{\partial h_p}{\partial t} + \rho_c \frac{\partial h_c}{\partial t} - \rho_c h_c \frac{\partial \varepsilon_p}{\partial t} - \varepsilon_p\rho_c \frac{\partial h_c}{\partial t} \tag{13}$$

Differentiating Equations 11 and 12, and knowing that the enthalpy of formation of the gases is constant, Equation 14 is obtained

$$\frac{\partial h_p}{\partial t} = Cp_p \frac{\partial T}{\partial t} \tag{14a}$$

and

$$\frac{\partial h_c}{\partial t} = Cp_c \frac{\partial T}{\partial t} \tag{14b}$$

Calculating ε_p from Equation 9 and differentiating

$$\frac{\partial \varepsilon_p}{\partial t} = \frac{1}{\rho_p - \rho_c}\frac{\partial \rho}{\partial t} \tag{15}$$

In order to obtain the enthalpy variation velocity as a function of temperature and rate of decomposition, Equations 14 and 15 are substituted into Equation 13, namely

$$\frac{\partial(\rho h)_y}{\partial t} = \frac{\rho_p h_p - \rho_c h_c}{\rho_p - \rho_c}\frac{\partial \rho}{\partial t} + \rho Cp\frac{\partial T}{\partial t} \tag{16}$$

in which ρCp is indicated as a weighted average of the reacted and unreacted properties: $\rho C_p = \rho_p \varepsilon_p Cp_p + (1-\varepsilon_p)\rho_c Cp_c$.

Now, it is possible to substitute these terms into the conservation of energy, Equation 8, where the left-hand side will then become

$$\frac{\partial \rho h S}{\partial t} = \rho h\frac{\partial S}{\partial t} + S\frac{\rho_p h_p - \rho_c h_c}{\rho_p - \rho_c}\frac{\partial \rho}{\partial t} + \rho Cp\frac{\partial T}{\partial t} \tag{17}$$

The third term of Equation 7 can then be written as

$$\frac{\partial \dot{m} h_g}{\partial y} = \dot{m}\frac{\partial h_g}{\partial y} + h_g\frac{\partial m_g}{\partial y} \tag{18}$$

The mass balance (Equation 3) can be substituted into Equation 18, to obtain

$$\frac{\partial \dot{m} h_g}{\partial y} = \dot{m} g\frac{\partial h_g}{\partial y} + h_g S\frac{\partial \rho}{\partial t} \tag{19}$$

Finally, the complete model equation can be obtained by substituting Equations 17 and 19 into the energy balance (Equation 7)

$$\rho Cp\frac{\partial T}{\partial t} = -\bar{h}\frac{\partial \rho}{\partial t} + \frac{1}{S}\frac{\partial}{\partial y}\left(kS\frac{\partial T}{\partial y}\right) + \dot{m} g\frac{\partial h_g}{\partial y} + h_g\frac{\partial \rho}{\partial t} \tag{20}$$

where h_g represents the enthalpy of gases, and $\bar{h}$ represents

$$\dot{h} = \frac{\rho_p h_p - \rho_c h_c}{\rho_p - \rho_c} \tag{21}$$

In order to solve this equation, it is necessary to calculate many parameters [11–13], such as the enthalpy of the gases, thermal conductivity, specific heat, and rate of degradation, i.e. the reaction kinetics. The methods required to obtain these parameters will be described in the following section.

3.2. Enthalpy of the pyrolysis gases

In Equation 20 there are two terms that contain the derivative of the density with respect to the time. In order to solve this equation, the values of the specific enthalpies $\bar{h}$ and h_g must be calculated and therefore it is necessary to calculate the enthalpies of formation of the non-reacted material, of the char, and of the outgoing gases. This calculation is very complicated because it requires exact knowledge of the chemical compositions of the starting material and of the final decomposition products. Grouping the two elements of Equation 20 containing the time derivative of the density, the following term is obtained

$$\frac{\partial \rho}{\partial t}(h_g - \bar{h}) \tag{22}$$

A method to overcome all the problems related with the calculation of each single specific formation enthalpy value is proposed here through the direct calculation of the term $(h_g - \bar{h})$. Differential thermal analysis together with thermogravimetric analysis can provide such a measure, on the basis of the following procedure being observed.

One of the hypotheses for the model is that the volume is constant during the reaction

$$p = c + g \tag{23}$$

where we indicate the unreacted material by p, the char by c, and the gases by g, the total enthalpy, ΔH, of the reaction can be expressed as

$$\Delta H = m_p h_p - m_c h_c - m_g h_g \tag{24}$$

Dividing Equation 24 by the total volume, V, and remembering that the mass of gases is equal to $(m_p - m_c)$ we obtain

$$\frac{\Delta H}{V} = \rho_p h_p - \rho_c h_c - (\rho_p - \rho_c)h_g \tag{25}$$

Dividing Equation 25 by $(\rho_p - \rho_c)$, and knowing that the product $V(\rho_p - \rho_c)$ is equal to $(m_p - m_c)$, yields

$$\frac{\Delta H}{m_p - m_g} = \frac{\rho_p h_p - \rho_c h_c}{\rho_p - \rho_c} - h_g = \bar{h} - h_g \tag{26}$$

This expression leads to the calculation of the term $\bar{h} - h_g$, using simple thermal analysis techniques. In fact, the left-hand side of Equation 26 represents the heat of ablation obtained in Part I [1] by simultaneous thermal analysis.

The time derivative of the density can be directly related to the decomposition kinetics of the material analyzed in the former study [1, 14]. The variation of the degree of decomposition in terms of density changes, required in the model Equation 20, can be easily computed using the following relationship

$$\frac{\partial \rho}{\partial t} = (\rho_0 - \rho_f)\frac{\partial \alpha}{\partial t} \tag{27}$$

This expression holds if the small volume change eventually occurring during the decomposition is neglected. Therefore, Equation 27 can be directly substituted in Equation 20 using, for the term $\partial\alpha/\partial t$, Equations 8 and 9 developed in the previous paper [1].

3.3. Testing the simulation program

The last part of this work is dedicated to the numerical testing of the simulation model. All the experimental data and model equations obtained are now used in a computer program in order to predict the temperature profile inside a sample of ablative material as a function of a given heat flux imposed on its surface.

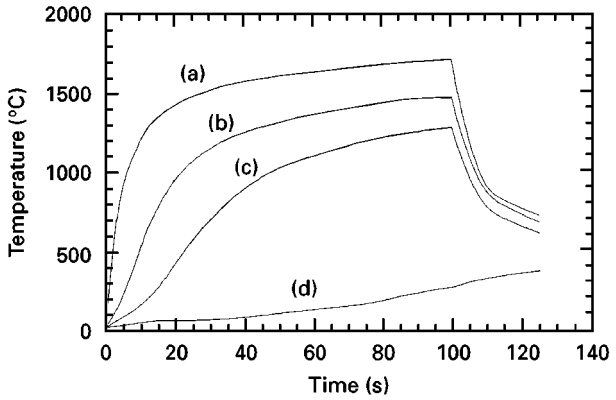

Figure 4 Calculated temperature profile corresponding to different thicknesses: (a) 0.7 mm, (b) 2.11 mm, (c) 3.51 mm, (d). 9.93 mm

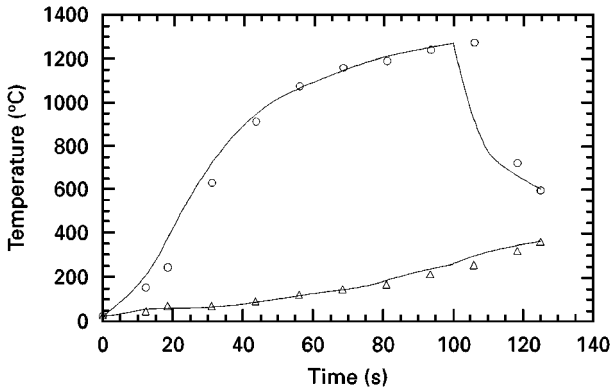

Figure 5 Comparison of the results of (——) the model and the arc test in relation to two different thicknesses: (○) 3.51 mm, (△) 9.93 mm.

A finite difference method is used to solve the mass and energy balance, and implemented on a workstation, the boundary conditions were obtained by imposing the heat flux on the surface, while the parameters used in the solution were calculated using the method proposed.

Figs 4 and 5 show the result of such an analysis compared with the experimental data obtained by the tests. It is possible to observe that a good correlation between the model and the experimental result is obtained. Although the description of the problem was simplified, this methodology was used with success for material selection, providing many indications of the behaviour of ablative systems, such as performance characteristic, temperature profiles, and thickness calculation.

4. Conclusions

The behaviour of a space protection system was modelled and the energy and mass balance equations were applied to a flat geometry, in order to obtain a model to simulate the behaviour of an ablative shield. As most of the parameters needed in this model were related to the thermal properties of the polymeric matrices and components of the ablative composite, traditional techniques discussed in Part I were used to obtain the parameters for a commercial ablative system. The mathematical model was tested with plasma arc techniques in order to confirm the validity of the results obtained, and to develop simple tools that allow simulation of a process for the design of the thickness of a thermal shield. An attempt was made in both parts of this work to simplify the description of a process which, due to the many variables involved, is somewhat complex and difficult to study.

Acknowledgements

The authors acknowledge the collaboration of Alenia S.pA. and Professor Nicolais, Department of Material and Production Engineering, University of Naples.

References

1. L. TORRE, J. M. KENNY and A. M. MAFFEZZOLI, *J. Mater. Sci.* **33** (1998) 000–000
2. G. F. D'ALELIO and J. A. PARKER (Eds) "Ablative plastics" (Marcel Dekker, New York, 1971).
3. E. L. STRAUSS, *Chem. Eng. Prog. Sym. Ser.* **59** (1963) 232.
4. A. TRIVISANO, S. PUZZIELLO, J. M. KENNY and L. NICOLAIS, in "Composite materials", edited by A. T. Di Benedetto, L. Nicolais and R. Watanabe (Elsevier, Amsterdam, 1992).
5. A. A. HILTZ, D. E. FLORENCE and D. L. LOWE, *J. Spacecraft* **5** (1968) 11.
6. E. M. LISTON, in "Ablative plastics", edited by G. F. D'Alelio and J. A. Parker (Marcel Dekker, New York, 1971) p. 379.
7. R. B. BIRD, N. L. STEWART and E. N. LIGHTFOOT, "Transport phenomena" (Wiley, New York, 1960).
8. J. R. WELTY, C. E. WICK and R. E. WILSON, "Fundamentals of momentum, heat, and mass transfer" (Wiley, New York, 1984).
9. J. COLLINS, O. SALMASSY and L. McALISTER, in "*Application of plastic material in aerospace*", edited by D. Simkins, (American Institute of Chemical Engineering, New York, NY, 1963) p. 9.
10. J. J. CARBERRY, "Chemical and catalytic reaction engineering" (McGraw-Hill, New York, 1976).
11. E. L. STRAUSS, in "Aspect of polymer degradation and stabilization", edited by H. H. G. Jellinek (Elsevier, New York, 1978) p. 528.
12. E. L. STRAUSS, *J. Spacecraft* **10** (1967) 1304.
13. Y. KANNO, *ICCM9* International Conference on Composite Materials (Edited by A. Mirarcte, Woodhead Publishing, Cambridge, 1993) p. 120.
14. J. M. KENNY, L. TORRE and L. NICOLAIS, *Thermochim. Acta* **227** (1993) 97.

Received 10 December 1996
and accepted 18 March 1998